







Characterization of cerebellar electrocortical dynamics under ether anesthesia in rats: a preliminary study using linear spectral and non-linear fractal analyses

 Jelena Podgorac Kojadinović^{1,*},  Branka Petković¹,  Aleksandar Kalauzi²,  Ljiljana Martać¹,  Slobodan Sekulić^{3,4} and  Gordana Stojadinović¹

¹*Department of Neurophysiology, Institute for Biological Research “Siniša Stanković” – National Institute of the Republic of Serbia, University of Belgrade, Bulevar despota Stefana 142, 11108 Belgrade, Serbia*

²*Department for Life Sciences, Institute for Multidisciplinary Research, University of Belgrade, Kneza Višeslava 1, 11030 Belgrade, Serbia*

³*Faculty of Medicine, University of Novi Sad, Hajduk Veljkova 3, 21000 Novi Sad, Serbia*

⁴*Department of Neurology, Clinical Center of Vojvodina, Hajduk Veljkova 1-7, 21000 Novi Sad, Serbia*

*Corresponding author: jelena.podgorac@ibiss.bg.ac.rs

Received: March 10, 202; **Revised:** April 21, 2025; **Accepted:** April 22, 2025; **Published online:** April 30, 2026

Abstract: The temporal evolution of cerebellar electrocortical activity during emergence from ether anesthesia was investigated using both linear and non-linear analytical methods. Adult male rats underwent operative craniotomy and implantation of a 16-channel microelectrode array targeting the paravermal cerebellar cortex. Following a 7-day recovery period, animals were exposed to ether via inhalation, and cerebellar electrocortical signals were recorded using a wireless acquisition system. Data were quantified through relative spectral power (RSP) across defined frequency bands, Higuchi's fractal dimension (HFD), and the Hurst exponent (H). A transitional phase between anesthetic depths was identified between the 17th and 19th min post-exposure. This period was characterized by a significant increase in RSP within low-frequency bands and a corresponding decrease in high-frequency bands beginning at the 17th min. Additionally, a marked decrease in HFD and an increase in H were observed at the 19th min, followed by a moderate rebound in HFD and a reduction in H. These findings suggest that non-linear dynamic measures, particularly HFD and H, may offer greater temporal precision in identifying the onset of awakening compared to conventional spectral analysis, highlighting their potential utility in monitoring anesthetic depth.

Keywords: ether anesthesia, cerebellum, electrocortical activity, wireless recording

Abbreviations: BIS – bispectral index; ECoG – electrocorticography; EEG – electroencephalography; GABA – γ -aminobutyric acid; HFD – Higuchi's fractal dimension; H – Hurst exponent; MEA – microelectrode array; NMDA – N-methyl-D-aspartate; RSP – relative spectral power

INTRODUCTION

As a general anesthetic, ether was first established in a Massachusetts hospital in 1846 [1]. Since then, various types of anesthetics, including administration by inhalation and intravenous delivery, have been introduced into medical practice and exhibit different pharmacokinetics and pharmacodynamic mechanisms. Despite their modes of action, these anesthetics achieve the same functional outcomes, including amnesia, unconsciousness, analgesia, and immobility [2]. Electroencephalography (EEG), which reflects neural activity, is a valuable tool

for assessing the effects of anesthetic depth on synaptic activity that influences higher cortical processing. An algorithm designed to monitor anesthetic depth through linear and non-linear signal analyses could be used to assess EEG patterns from various brain regions. However, non-linear measures like Higuchi's fractal dimension (HFD) and dimensional complexity may provide advantages over traditional linear measures in quantifying anesthetic effects on brain activity, particularly concerning subtle changes in cortical and cerebellar dynamics. For example, the non-linear measure of dimensional

complexity correlates better with anesthetic depth than the linear spectral edge frequency [3]; different anesthetics affect spectral entropy and HFD differently across brain regions and frequency bands [4]. HFD is a more stable measure than third-order correlation, as confirmed by surrogate data tests for nonlinearity in cerebellar signals in a brain injury model [5]. Different anesthetics also create unique brain dynamics when HFD measures anesthesia depth [6]. EEG signals obtained from patients under deeper levels of anesthesia become more ordered and less chaotic. By measuring the dimensionality of EEG through non-linear parameters, consciousness could be evaluated through the lens of deterministic chaos in the brain [7].

During general anesthesia, the brain experiences various altered states of consciousness, depending on the type and dosage of administered anesthetic agents. These states are typically categorized as unconsciousness, disconnected and connected consciousness [8]. A key mechanism underlying the transition to unconsciousness involves the disruption of functional connectivity, particularly in the posterior parietal cortex [9]. Conscious experience is generally understood to emerge from complex information processing within widespread cerebral networks.

Although the cerebellum is not traditionally included among the core neural correlates of consciousness [13], growing evidence suggests that it plays a modulatory role. The cerebellum maintains reciprocal connections with the cerebral cortex via the thalamus and pons [10,11] and contributes to processing of emotional and sensorimotor information across both conscious and unconscious states. Distinct levels of awareness are associated with the generation of intrinsic brain models that facilitate predictive timing and influence autonomic responses, potentially altering unconscious emotional states [12].

The cerebellum's role in consciousness remains a topic of debate. Some studies suggest that its influence is minimal due to the organization of its intrinsic circuitry [14], and others indicate distinct cerebellar activation patterns during awakening, implicating its involvement in re-establishing conscious processing [15].

Despite the introduction of ether into clinical practice over 170 years ago, the molecular mechanisms underlying its anesthetic effects, particularly its role in

modulating consciousness, continue to be an area of active investigation. Ether acts by potentiating inhibitory neurotransmission through γ -aminobutyric acid (GABA) and glycine receptors, and two-pore domain potassium (2P) channels. It simultaneously suppresses excitatory neurotransmission by inhibiting N-methyl-D-aspartate (NMDA) and glutamate receptors [16]. Additional targets include nicotinic acetylcholine receptors, serotonin type 3 receptors, and neuronal pacemaker current channels.

Research on ether's effects on brain activity has largely focused on the cerebrum, with relatively little attention paid to cerebellar dynamics during anesthesia [17-20]. In this context, the present study aims to investigate the temporal pattern of changes in cerebellar electrocorticographic (ECoG) activity following ether administration. To achieve this, a combination of linear and non-linear analytical measures, including relative spectral power (RSP) in defined frequency bands, Higuchi's fractal dimension (HFD), and the Hurst exponent (H) was employed. These parameters were utilized to assess the depth of anesthesia and determine the timing of emergence from the anesthetized state.

Integrating these analytical methods into anesthetic depth monitoring has the potential to improve the clinical assessment of consciousness levels [21]. Although bispectral index (BIS) monitoring is widely used in perioperative practice, it lacks the granularity needed to detect the precise moment when awareness is regained [22]. Non-linear dynamic measures such as HFD and H may offer greater sensitivity in identifying this critical transition, providing a valuable complement to existing monitoring tools.

MATERIALS AND METHODS

Ethics statement

All animal procedures complied with Directive 2010/63/EU on the protection of animals used for experimental and other scientific purposes and were approved by the Ethical Committee for the Use of Laboratory Animals of the Institute for Biological Research "Siniša Stanković", University of Belgrade, Serbia.

Animals

The experiments were performed on 4 adult (2-2.5-month old) male Wistar rats. They were housed in the animal facility of the Institute for Biological Research “Siniša Stanković”, Belgrade, Serbia under standard conditions (12-h light-dark cycle, temperature of about 21-24°C). Before surgery, they were housed in standard plexiglass cages with soft bedding and food and water available *ad libitum*. Post-operatively, they were transferred to cages with a higher cover top.

Implantation surgery

Surgical procedures were carried out in an aseptic environment using sterilized surgical tools. Animals were anesthetized by intraperitoneal administration of Zoletil 50 (Virbac, Carros, France) at a dose of 50 mg/kg (dissolved in normal saline (0.9% NaCl) and fixed in a stereotaxic frame for the surgical procedure. A midline incision was made, and the entire skull surface was exposed and freed from connective tissue. Dorsal cranial muscles were removed to expose the caudal part of the skull and the first cervical vertebrae. The squamous part of the occipital bone associated with the bregma (AP: -9.0, -12.0; R/L=1.0) was removed to make a 4x3 mm opening over the cerebellum. A dental drill was used for the craniotomy. A temporary saline drip was installed to keep the dura moist. The tip of a 29-gauge injection needle was bent at a 90° angle and used as a micro knife to incise, reflect, and remove the dura. Immediately after dura removal, warm (35°C) AGAR (2% in 0.1 M phosphate-buffered saline; Sigma-Aldrich, MA, USA) was placed over the exposed cerebellar surface. Before the microelectrode carrier was placed in the final position, one copper wire (ground) was placed under the skull through the hole in the skull. The 16-channel microelectrode array (MEA) was implanted at the paravermal cerebellar cortex at stereotaxic coordinates for the bregma: AP: -9.0, -12.0; R/L=1.0; H: -3.5 (mm) using a standard Kopf micro positioner (David Kopf Instruments, CA, USA) and the flattened surface of the silicon cover was lowered until it touched and leveled the cerebellar surface so that the cerebellar cortex was stabilized and its curvature reduced. The 18-pin Male Omnetics connector (Alpha Omega Engineering Ltd, Nazareth, Israel) was fixed to the skull with dental cement (Cegal N,

Galenika, Belgrade, Serbia). The skin incision was closed in layers, and surgical antibiotic powder (neomycin, Veterinarski Zavod Subotica, Subotica, Serbia) was spread over the head wound.

Ether administration and cerebellar ECoG activity registration

After recovery from surgery (on the 7th day), animals were exposed to ether (Sigma-Aldrich, MA, USA) presented on a cotton ball inside a transparent glass jar until they became unconscious (about 5 to 10 min). The effective ether concentration was 1.9% (0.08 mL per L of jar volume) [23]. Immediately after induction of ether anesthesia, cerebellar ECoG activities of the animals were recorded by the wireless acquisition system (Telespike, Alpha Omega Engineering Ltd, Nazareth, Israel) and quantified by calculating the RSP in defined frequency ranges, HFD, and H. Cerebellar ECoG signals were sequentially digitized at the sampling rate of 788 Hz and filtered to avoid artifacts due to movements and other non-brain sources of electric activity.

Calculation of relative power spectrum

We evaluated Fourier power spectra $P(f_i)$ and introduced a normalized power spectrum [24], according to the formula:

$$P_n(f) = \frac{P(f_i)}{\sum_{f_i} P(f_i)} \quad (1)$$

$$\sum_i P_i(f_i) = 1$$

Spectral power was calculated for each of the N=5 already defined frequency ranges – delta (0.125-4.0 Hz), theta (4.125-8.0 Hz), alpha (8.125-15.0 Hz), beta (15.125-32.0 Hz), and gamma (32.125-128.0 Hz). The Fourier epoch was defined as 8 s, setting low limits for each range. Finally, the corresponding eight Fourier power spectral components were averaged within each 1-Hz interval.

Calculation of Higuchi's fractal dimension

HFD was determined using the Higuchi algorithm [25-27]. For a discrete time series $\{x(1), x(2), \dots, x(N)\}$ new time series were created, according to the formula:

$$X_k^m : x(m), x(m+k), x(m+2k), \dots, x(m+\text{int}[(N-m)/k]k); m = 1, 2, \dots, k; \\ X_k^m = \{x(m), x(m+1), \dots, x(m+\text{int}[(N-m)/k]k)\} \{1, 2, \dots, k\}. \quad (2)$$

where m is the initial time, k is the time interval, $k = 2, \dots, k_{\max}$, $k \in \{1, 2, \dots, k_{\max}\}$ and $\text{int}(r)$ is the integer part of the real number r . The length $L_m(k)$ was computed for each of the X_k^m series or curves according to the formula:

$$L_m(k) = \frac{1}{k} \left[\sum_{i=1}^{\text{int} \left[\frac{N-m}{k} \right]} |x(m+ik) - x(m+(i-1)k)| \right] \frac{N-1}{\text{int} \left[\frac{N-m}{k} \right]} \quad (3)$$

and $L_m(k)$ was averaged for all m :

$$L(k) = \frac{\sum_{m=1}^k L_m(k)}{k} \quad (4)$$

giving the mean value of the curve length $L(k)$ for each $k = \{1, 2, \dots, k_{\max}\}$. Finally, HFD was determined from the plot $\log(L(k))$ versus $1/k$ as the slope of the straight line. We used epochs of 500 experimental points and $k_{\max} = 8$ [26]. Individual HFD values from all epochs were averaged to obtain a final HFD value for a particular signal.

Calculation of the Hurst exponent

The Hurst exponent for a time series of length N was determined by using rescaled range analysis [28], where a straight line is interpolated between points $\log \left(\frac{R(n)}{S(n)} \right) = f(\log(n))$, and its slope is used as H . Here $R(n)$ and $S(n)$ denote range and standard deviation, respectively, of a rescaled partial time series $n = N, N/2, N/4, \dots$

The scaling properties of a given discrete time series $X = \{X_1, X_2, \dots, X_N\}$ can be expressed through the dependence of the autocorrelation function $C(k)$ vs. the H in terms of a large-time lag, k :

$$C(k) = \frac{1}{N-k} \sum_{i=1}^{N-k} X_i \cdot X_{i+k} \sim k^{2H-2} \quad (5)$$

If $N \rightarrow \infty$, $\sum_{k=1}^N C(k) \rightarrow \infty$, then H is in the range 0.5-1,

and the process is called a long-range correlated one or a long-memory process [29]. A high value in the series will probably be followed by another high value. An H value in the range 0-0.5 indicates a time series with long-term switching between high and low values in adjacent pairs. A value of $H=0.5$ can indicate a completely uncorrelated series, typical for Brownian motion.

Statistical analysis

A preliminary Shapiro-Wilk test was conducted to assess the normality of the datasets for the RSP within defined frequency ranges, as well as HFD and H obtained at specific time points following ether anesthesia ($n = 4$ animals). Given that the data exhibited a normal distribution, repeated measures ANOVA was conducted, followed by a post hoc Fisher LSD test to analyze the temporal changes for each parameter.

RESULTS

Temporal pattern of the relative spectral power (RSP) in the cerebellum after ether anesthesia

Spectral analysis, a linear method for quantifying EEG, offers data on changes in spectral power density across specific frequency ranges. The analyzed linear measure (RSP) of cerebellar ECoG activity after ether anesthesia varied over time (Fig. 1). Repeated measures ANOVA indicated that the observed effect was significant for RSP in the delta ($F_{6,18}=5.61$, $P<0.01$), alpha ($F_{6,18}=3.64$, $P<0.05$), and beta ($F_{6,18}=3.70$, $P<0.05$) frequency ranges, while the theta and gamma frequency ranges were on the margin of statistical significance ($F_{6,18}=2.32$, $P=0.08$, and $F_{6,18}=2.39$, $P=0.07$, respectively). RSP in the delta frequency range (Fig. 1A) was dominant and exhibited a specific temporal pattern characterized by similar values from the 13th to the 15th min, a sudden significant increase in the 17th min, and a gradual decrease returning to previous values from the 19th to the 22nd min after ether anesthesia. RSP in the alpha (Fig. 1C), beta (Fig. 1D),

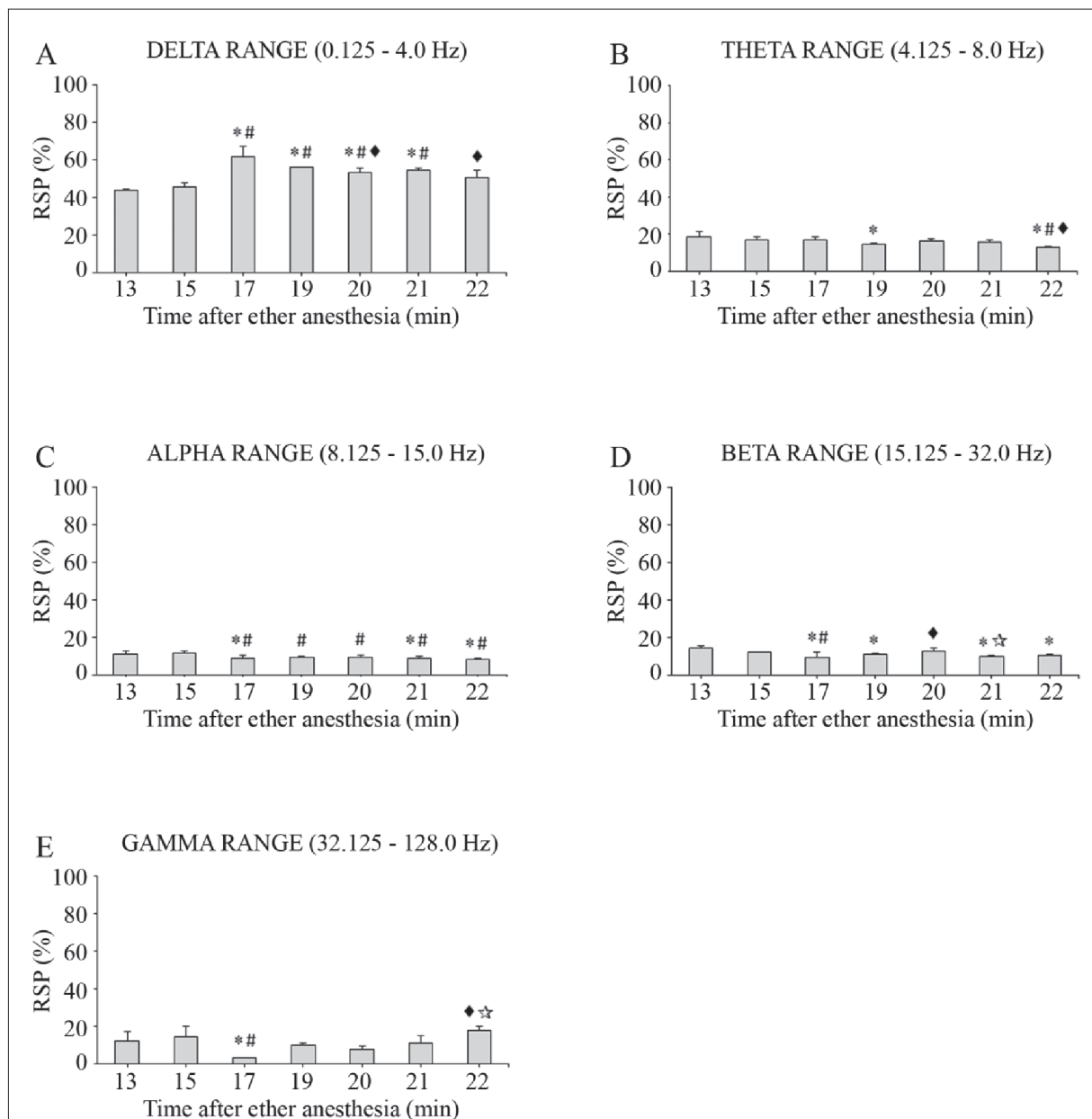


Fig. 1. The temporal pattern of the relative spectral power (RSP) in the delta (A), theta (B), alpha (C), beta (D), and gamma (E) frequency ranges in the cerebellum after ether anesthesia. Each bar represents the mean+SEM (n=4 animals). *P<0.05 vs. 13th min, #P<0.05 vs. 15th min, ♦P<0.05 vs. 17th min, and ☆ P<0.05 vs. 20th min (Fisher's LSD test).

and gamma (Fig. 1E) frequency ranges showed similar values and demonstrated a pattern contrary to that of delta, specifically a significant decrease in the 17th min and a gradual increase from the 19th to the 22nd min after ether anesthesia. RSP in the theta frequency range changed over time, exhibiting a significant decrease

in the 19th and 22nd min (Fig. 1B). These results indicate an increase in RSP in slow frequency ranges and a decrease in RSP in fast frequency ranges during the period from the 17th to the 22nd min after ether anesthesia, with the temporal dynamics of significant changes being specific to each frequency range.

Temporal pattern of Higuchi's fractal dimension and Hurst exponent in the cerebellum after ether anesthesia

In addition to basic spectral analysis, non-linear tools have an important place in the analysis of EEG signals related to dynamics and chaotic measures of complexity and stability. Non-linear measures, HFD and H, also exhibited significant differences over time ($F_{6,18}=4.08$, $P<0.01$, respectively) after ether anesthesia (Fig.2). Their temporal patterns showed a significant transitional decrease in HFD and increase in H in the 19th min, followed by a more moderate but persistent increase in HFD and decrease in H after the 19th min, indicating that the system acquired a more complex state than before the 19th min. These results showed that cerebellar electrocortical activity becomes less predictable, more complex, and more chaotic as the depth of ether anesthesia decreases over time, with the 19th min clearly defined as the time of “awakening” after ether anesthesia.

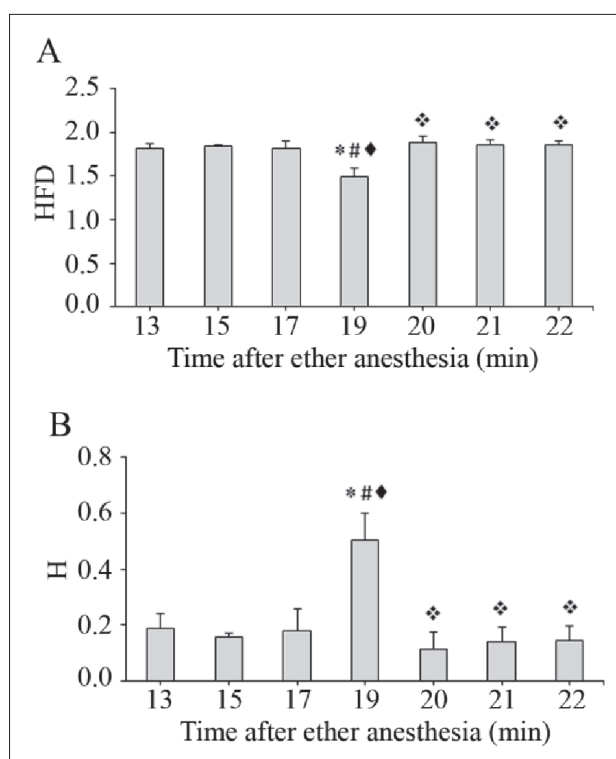


Fig. 2. The temporal pattern of Higuchi's fractal dimension – HFD (A), and Hurst exponent – H (B) in the cerebellum after ether anesthesia. Each bar represents the mean±SEM (n=4 animals). *P<0.05 vs. 13th min, #P<0.05 vs. 15th min, •P<0.05 vs. 17th min, and ◊P<0.05 vs. 19th min (Fisher's LSD test).

DISCUSSION

The central nervous system (CNS) exhibits complex and often unpredictable behavior under varying experimental conditions [30]. Although brain function is inherently chaotic, mathematical modeling has demonstrated that this complexity may follow deterministic patterns governed by non-linear dynamics. Advances in non-linear signal processing, particularly the application of measures such as Higuchi's fractal dimension (HFD) and the Hurst exponent (H), have provided valuable insights into the operational principles of brain networks [21,31]. These measures have proven useful in understanding the chaotic nature of brain activity but also as potential indicators of anesthetic depth, complementing traditional spectral power analyses [32,33].

Waveform morphology in electroencephalographic (EEG) recordings is known to be specific to different anesthetic agents. A general pattern has been observed: increasing anesthetic depth is typically associated with EEG slowing [34]. Under agents such as propofol or volatile anesthetics, alpha activity diminishes while theta and delta waves become predominant [34,35]. High-frequency gamma oscillations, which are implicated in higher cognitive processing, are significantly reduced under isoflurane anesthesia in a dose-dependent manner, correlating with the onset of unconsciousness [36]. Sevoflurane, another volatile anesthetic, has been shown to induce dose-dependent EEG changes in experimental studies on adult Sprague-Dawley rats [37]. At lower concentrations, sevoflurane increases beta and low-gamma power in the prefrontal cortex and central thalamus, while at higher concentrations it enhances slow-delta power and delta coherence across these regions.

Importantly, the loss of consciousness is also associated with a decline in HFD, reflecting a reduction in EEG complexity [38,39]. While EEG is often interpreted as a measure of cortical function, it also reflects subcortical activity [40]. The cerebellum is a distinct and highly organized region of the brain. Despite its primary association with motor control, it has increasingly been recognized for its roles in cognition, language, emotion, and various psychiatric and neurodevelopmental disorders [41]. Anatomically, the cerebellum contains 4-5 times more neurons than the cerebral cortex and is characterized by an equally

rich and intricate network of extrinsic connections. Even in the absence of external stimuli, as in sleep or anesthesia, the cerebellar cortex generates slow intrinsic oscillations [42].

Our previous study demonstrated that administration of different anesthetics (nembutal, ketamine, and zoletil) resulted in cerebellar activity dominated by delta frequency oscillations, accompanied by reduced spectral entropy in the beta range [4]. The findings of the present study align with these observations, showing a progressive decrease in delta activity and a concurrent increase in gamma activity in the cerebellum following ether anesthesia. Specifically, the emergence from anesthesia, observed around the 17th min, was marked by a significant reduction in alpha and delta power, fluctuating beta activity, and a slight decline in theta power.

Alpha coherence is known to disrupt cortico-subcortical communication, particularly within the thalamocortical circuits [43], and both alpha and delta bands dominate during propofol-induced anesthesia [35]. Oscillatory activity within cerebellar circuits occurs across both low- and high-frequency bands [44]. Golgi interneurons contribute to theta band resonance [45], while Purkinje cells generate slow complex spikes that participate in theta and beta oscillations originating in the inferior olive and cerebellar granular layer [44]. The presence of slow theta activity is particularly associated with deep sleep and attentive states [45].

Quantitative measures of EEG complexity (HFD) and persistence or long-term memory (H) demonstrated temporal patterns consistent with spectral data, albeit with a slight lag. Prior to and after the significant change in brain activity at the 19th min, both HFD and H showed relative stability, followed by a decrease in HFD and an increase in H. Lower HFD values suggest dominant delta and theta activity, while higher HFD values indicate increased high-frequency EEG components [46,47]. Interestingly, while reduced signal complexity (lower HFD) is often associated with higher amplitude signals in the lower frequency ranges [46,48], this relationship manifested with a temporal discrepancy occurring around the 17th min for spectral changes and the 19th min for non-linear measures.

After the 19th min, both delta power and HFD values increased. This apparent paradox may be attributed

to the contribution of additional frequency bands, particularly theta, alpha, and low beta, to overall signal complexity. These “middle” frequency ranges may modulate HFD in complex ways [38,48], reinforcing the complementary value of spectral and non-linear analyses in characterizing brain activity under anesthesia.

Despite the robustness of the findings, this study has limitations. Artifacts such as signal noise, potentially introduced by high electrode resistance or muscle activity during the recovery phase, must be considered, particularly during the awakening period when movement artifacts are more likely to occur.

CONCLUSIONS

These findings indicate that temporal patterns of the analyzed linear and non-linear measures of cerebellar ECoG activity could be useful in recognizing different conditions (unconsciousness, disconnected consciousness, and connected consciousness) and anesthetic depth during recovery from anesthesia. Moreover, they identified the 17th to the 19th min after ether anesthesia as the period in which different levels of anesthesia transitioned. This period can be seen as crucial for the level of consciousness or the transition between deep anesthesia with loss of consciousness and transient consciousness. It is also worth noting that non-linear measurements (HFD and H) provide a more accurate time of “awakening” than linear measurements (RSP) after ether anesthesia. To confirm this hypothesis, further studies are required that involve monitoring cerebellar electrocortical activity in a larger population of animals.

Funding: This study was supported by the Ministry of Science, Technological Development and Innovation of the Republic of Serbia (Contract No. 451-03-136/2025-03/200007).

Acknowledgments: We thank Dr. Milka Čulić for introducing and providing the wireless acquisition system. The results presented in this manuscript are in line with Sustainable Development Goal 3 (Good Health and Well-being) of the United Nations 2030 Agenda.

Author contributions: Conceptualization, methodology, JPK, and GS; formal analysis, AK, and GS; investigation, JPK, LM, and GS; writing – original draft preparation, JPK; writing – review and editing, BP, AK, and SS; visualization, BP. All authors have read and agreed to the published version of the manuscript.

Conflict of interest disclosure: The authors declare that they have no conflict of interest.

Data availability: The raw data underlying this article is available as an online supplementary research dataset: https://www.serbio-soc.org.rs/NewUploads/Uploads/Podgorac%20Kojadinovic%20et%20al_Dataset.pdf

REFERENCES

- Hudetz AG, Mashour GA. Disconnecting consciousness: Is there a common anesthetic end point? *Anesth Analg*. 2016;123(5):1228-40. <https://doi.org/10.1213/ANE.0000000000001353>
- Son Y. Molecular mechanisms of general anesthesia. *Korean J Anesthesiol*. 2010;59(1):3-8. <https://doi.org/10.4097/kjae.2010.59.1.3>
- Van den Broek PLC, Van Egmond J, Van Rijn CM, Dirksen R, Coenen AML, Booij LHDJ. The application of a non-linear analysis technique to the monitoring of anesthetic effects in the rat. In: Lehnertz K, Arnhold J, Grassberger P, editors. *Proceedings of the Workshop: Chaos in brain?*; 1999 Mar 10-12; Bonn, Germany. World Scientific;2000. p. 259-62. https://doi.org/10.1142/9789812793782_0027
- Kekovic G, Stojadinovic G, Martac L, Podgorac J, Sekulic S, Culic M. Spectral and fractal measures of cerebellar and cerebral activity in various types of anesthesia. *Acta Neurobiol Exp (Wars)*. 2010;70(1):67-75. <https://doi.org/10.55782/ane-2010-1775>
- Spasic S. Surrogate data test for nonlinearity of the rat cerebellar electrocorticogram in the model of brain injury. *Signal Process*. 2010;90(12):3015-25. <https://doi.org/10.1016/j.sigpro.2010.04.005>
- Spasic S, Kesic S, Kalauzi A, Saponjic J. Different anesthesia in rat induces distinct inter-structure brain dynamic detected by Higuchi fractal dimension. *Fractals – Complex Geometry Patterns and Scaling in Nature and Society*. 2011;19(1):113-23. <https://doi.org/10.1142/S0218348X1100521X>
- Klonowski W, Stepien P, Stepien R. Complexity measures of brain electrophysiological activity: In consciousness, under anesthesia, during epileptic seizure, and in physiological sleep. *J Psychophysiol*. 2010;24(2):131-5. <https://doi.org/10.1027/0269-8803/a000024>
- Bonhomme V, Staquet C, Montupil J, Defresne A, Kirsch M, Martial C, Vanhaudenhuyse A, Chatelle C, Larroque SK, Raimondo F, Demertzi A, Bodart O, Laureys S, Gosseries O. General anesthesia: A probe to explore consciousness. *Front Syst Neurosci*. 2019;13:36. <https://doi.org/10.3389/fnsys.2019.00036>
- Alkire MT, Hudetz AG, Tononi G. Consciousness and anesthesia. *Science*. 2008;322(5903):876-80. <https://doi.org/10.1126/science.1149213>
- Herculano-Houzel S. The human brain in numbers: a linearly scaled-up primate brain. *Front Hum Neurosci*. 2009;3:31. <https://doi.org/10.3389/neuro.09.031.2009>
- Herculano-Houzel S. Coordinated scaling of cortical and cerebellar numbers of neurons. *Front Neuroanat*. 2010;4:12. <https://doi.org/10.3389/fnana.2010.00012>
- Clausi S, Iacobacci C, Lupo M, Olivito G, Molinari M, Leggio M. The role of the cerebellum in unconscious and conscious processing of emotions: A review. *Appl Sci*. 2017;7(5):521. <https://doi.org/10.3390/app7050521>
- Tononi G, Koch C. Consciousness: here, there and everywhere?. *Philos Trans R Soc Lond B Biol Sci*. 2015;370(1668):20140167. <https://doi.org/10.1098/rstb.2014.0167>
- Tononi G. Consciousness, information integration, and the brain. *Prog Brain Res*. 2005;150:109-26. [https://doi.org/10.1016/S0079-6123\(05\)50009-8](https://doi.org/10.1016/S0079-6123(05)50009-8)
- Dorokhov VB, Malakhov DG, Orlov VA, Ushakov VL. Experimental model of study of consciousness at the awakening: FMRI, EEG and behavioral methods. In: Samsonovich A, editor. *Biologically Inspired Cognitive Architectures 2018. BICA 2018. Advances in Intelligent Systems and Computing Vol. 848*. Cham: Springer; 2019. p. 82-7. https://doi.org/10.1007/978-3-319-99316-4_11
- Forman SA, Chin VA. General anesthetics and molecular mechanisms of unconsciousness. *Int Anesthesiol Clin*. 2008;46(3):43-53. <https://doi.org/10.1097/AIA.0b013e3181755da5>
- Dow RS. The electrical activity of the cerebellum and its functional significance. *J Physiol*. 1938;94(1):67-86. <https://doi.org/10.1113/jphysiol.1938.sp003663>
- Swank RL, Watson CW. Effects of barbiturates and ether on spontaneous electrical activity of dog brain. *J Neurophysiol*. 1949;12(2):137-60. <https://doi.org/10.1152/jn.1949.12.2.137>
- Domino EF, Ueki S. Differential effects of general anesthetics on spontaneous electrical activity of neocortical and rhinencephalic brain systems of the dog. *J Pharmacol Exp Ther*. 1959;127:288-304.
- Persson A, Peterson E, Wählin A. EEG-changes during general anaesthesia with enflurane (Efrane) in comparison with ether. *Acta Anaesthesiol Scand*. 1978;22(4):339-48. <https://doi.org/10.1111/j.1399-6576.1978.tb01309.x>
- Jameson LC, Sloan TB. Using EEG to monitor anesthesia drug effects during surgery. *J Clin Monit Comput*. 2006;20(6):445-72. <https://doi.org/10.1007/s10877-006-9044-x>
- Johansen JW. Update on bispectral index monitoring. *Best Pract Res Clin Anaesthesiol*. 2006;20(1):81-99. <https://doi.org/10.1016/j.bpa.2005.08.004>
- Johns Hopkins University, Animal Care and Use Committee [Internet]. Baltimore (MD): Johns Hopkins University; [Revised by the JHU Joint Health Safety and Environment/ Animal Care and Use Committee 2006 Feb 22; cited 2025 Apr 29]. Use of Ether for Animal Anesthesia; [reviewed 9/25/13, 1/31/18, 1/15/21]. Available from: <https://animal-care.jhu.edu/wp-content/uploads/sites/5/Ether-for-Animal-Anesthesia.pdf>
- Quiroga RQ, Arnhold J, Grassberger P. Learning driver-response relationships from synchronization patterns. *Phys Rev E Stat Phys Plasmas Fluids Relat Interdiscip Topics*. 2000;61(5 Pt A):5142-8. <https://doi.org/10.1103/physreve.61.5142>
- Higuchi T. Approach to an irregular time series on the basis of the fractal theory. *Physica D*. 1988;31(2):277-83. [https://doi.org/10.1016/0167-2789\(88\)90081-4](https://doi.org/10.1016/0167-2789(88)90081-4)

26. Spasic S, Kalauzi A, Grbic G, Martac L, Culic M. Fractal analysis of rat brain activity after injury. *Med Biol Eng Comput.* 2005;43(3):345-8. <https://doi.org/10.1007/BF02345811>
27. Klonowski W, Olejarczyk E, Stepień R, Jalowiecki P, Rudner R. Monitoring the depth of anaesthesia using fractal complexity method. In: Novak MN, editor. *Complexus mundi. emergent patterns in nature.* New Jersey, London, Singapore: World Scientific, 2006. p. 333-42. https://doi.org/10.1142/9789812774217_0031
28. Mandelbrot B, Wallis JR. Robustness of the rescaled range R/S in the measurement of noncyclic long-run statistical dependence. *Water Resour Res.* 1969;5(5):967-88. <https://doi.org/10.1029/WR005i005p00967>
29. Carbone A. Algorithm to estimate the Hurst exponent of high-dimensional fractals. *Phys Rev E Stat Nonlin Soft Matter Phys.* 2007;76(5 Pt 2):056703. <https://doi.org/10.1103/PhysRevE.76.056703>
30. Natarajan K, Acharya U R, Alias F, Tiboleng T, Puthusserypady SK. Nonlinear analysis of EEG signals at different mental states. *Biomed Eng Online.* 2004;3(1):7. <https://doi.org/10.1186/1475-925X-3-7>
31. Stam CJ. Nonlinear dynamical analysis of EEG and MEG: review of an emerging field. *Clin Neurophysiol.* 2005;116(10):2266-301. <https://doi.org/10.1016/j.clinph.2005.06.011>
32. Widman G, Schreiber T, Rehberg B, Hoeft A, Elger CE. Quantification of depth of anesthesia by nonlinear time series analysis of brain electrical activity. *Phys Rev E Stat Phys Plasmas Fluids Relat Interdiscip Topics.* 2000;62(4 Pt A):4898-903. <https://doi.org/10.1103/physreve.62.4898>
33. Otto KA. EEG power spectrum analysis for monitoring depth of anaesthesia during experimental surgery. *Lab Anim.* 2008;42(1):45-61. <https://doi.org/10.1258/la.2007.006025>
34. Hagihira S. Changes in the electroencephalogram during anaesthesia and their physiological basis. *Br J Anaesth.* 2015;115 Suppl 1:i27- i31. <https://doi.org/10.1093/bja/aev212>
35. Cartailleur J, Parutto P, Touchard C, Vallée F, Holcman D. Alpha rhythm collapse predicts iso-electric suppressions during anesthesia. *Commun Biol.* 2019;2:327. <https://doi.org/10.1038/s42003-019-0575-3>
36. Hudetz AG, Vizuite JA, Pillay S. Differential effects of isoflurane on high-frequency and low-frequency γ oscillations in the cerebral cortex and hippocampus in freely moving rats. *Anesthesiology.* 2011;114(3):588-95. <https://doi.org/10.1097/ALN.0b013e31820ad3f9>
37. Sorrenti V, Cecchetto C, Maschietto M, Fortinguerra S, Buri-ani A, Vassanelli S. Understanding the Effects of Anesthesia on Cortical Electrophysiological Recordings: A Scoping Review. *Int J Mol Sci.* 2021;22(3):1286. <https://doi.org/10.3390/ijms22031286>
38. Nguyen-Ky T, Wen P, Li Y. Monitoring the depth of anaesthesia using Hurst exponent and Bayesian methods. *IET Signal Process.* 2014;8(9):907-17. <https://doi.org/10.1049/iet-spr.2013.0113>
39. Varley TF, Craig M, Adapa R, Finoia P, Williams G, Allanson J, Pickard J, Menon DK, Stamatakis EA. Fractal dimension of cortical functional connectivity networks & severity of disorders of consciousness. *PLoS One.* 2020;15(2):e0223812. <https://doi.org/10.1371/journal.pone.0223812>
40. Daly I, Williams D, Hwang F, Kirke A, Miranda ER, Nasuto SJ. Electroencephalography reflects the activity of sub-cortical brain regions during approach-withdrawal behaviour while listening to music. *Sci Rep.* 2019;9(1):9415. <https://doi.org/10.1038/s41598-019-45105-2>
41. Phillips JR, Hewedi DH, Eissa AM, Moustafa AA. The cerebellum and psychiatric disorders. *Front Public Health.* 2015;3:66. <https://doi.org/10.3389/fpubh.2015.00066>
42. Ros H, Sachdev RN, Yu Y, Sestan N, McCormick DA. Neocortical networks entrain neuronal circuits in cerebellar cortex. *J Neurosci.* 2009;29(33):10309-20. <https://doi.org/10.1523/JNEUROSCI.2327-09.2009>
43. Purdon PL, Sampson A, Pavone KJ, Brown EN. Clinical electroencephalography for anesthesiologists: Part I: Background and basic signatures. *Anesthesiology.* 2015;123(4):937-60. <https://doi.org/10.1097/ALN.0000000000000841>
44. De Zeeuw CI, Hoebeek FE, Schonewille M. Causes and consequences of oscillations in the cerebellar cortex. *Neuron.* 2008;58(5):655-8. <https://doi.org/10.1016/j.neuron.2008.05.019>
45. Gandolfi D, Lombardo P, Mapelli J, Solinas S, D'Angelo E. θ -Frequency resonance at the cerebellum input stage improves spike timing on the millisecond time-scale. *Front Neural Circuits.* 2013;7:64. <https://doi.org/10.3389/fncir.2013.00064>
46. Spasic S, Kalauzi A, Kesic S, Obradovic M, Saponjic J. Surrogate data modeling the relationship between high frequency amplitudes and Higuchi fractal dimension of EEG signals in anesthetized rats. *J Theor Biol.* 2011;289:160-6. <https://doi.org/10.1016/j.jtbi.2011.08.037>
47. Zappasodi F, Marzetti L, Olejarczyk E, Tecchio F, Pizzella V. Age-related changes in electroencephalographic signal complexity. *PLoS One.* 2015;10(11):e0141995. <https://doi.org/10.1371/journal.pone.0141995>
48. Kalauzi A, Bojić T, Vuckovic A. Modeling the relationship between Higuchi's fractal dimension and Fourier spectra of physiological signals. *Med Biol Eng Comput.* 2012;50(7):689-99. <https://doi.org/10.1007/s11517-012-0913-9>

ONLINE SUPPLEMENTARY RESEARCH DATASET

The raw data underlying this article is available as an online supplementary research dataset: https://www.serbiosoc.org.rs/NewUploads/Uploads/Podgorac%20Kojadinovic%20et%20al_Dataset.pdf